PLOS ONE

RESEARCH ARTICLE

Improved cognition impairment by activating cannabinoid receptor type 2: Modulating CREB/BDNF expression and impeding TLR-4/NFκBp65/M1 microglia signaling pathway in D-galactose-injected ovariectomized rats

Sahar S. Abd El-Rahman[1]*, **Hany M. Fayed**[2]

1 Department of Pathology, Faculty of Veterinary Medicine, Cairo University, Giza, Egypt, **2** Pharmacology Department, Medical Research and Clinical Studies Institute, National Research Centre, Dokki, Giza, Egypt

* saharsamirmah@cu.edu.eg, saharsamirmah@hotmail.com

Citation: Abd El-Rahman SS, Fayed HM (2022) Improved cognition impairment by activating cannabinoid receptor type 2: Modulating CREB/BDNF expression and impeding TLR-4/NFκBp65/M1 microglia signaling pathway in D-galactose-injected ovariectomized rats. PLoS ONE 17(3): e0265961. https://doi.org/10.1371/journal.pone.0265961

Editor: Cristoforo Scavone, Universidade de Sao Paulo, BRAZIL

Received: September 17, 2021

Accepted: March 10, 2022

Published: March 29, 2022

Data Availability Statement: All relevant data are within the paper and its Supporting information files.

Funding: The author(s) received no specific funding for this work.

Competing interests: The authors have declared that no competing interests exist.

Abstract

Alzheimer's disease (AD) is characterized by an active inflammatory response induced by the brain's deposition and accumulation of amyloid-beta (Aβ). Cannabinoid receptor type 2 (CB2R) is expressed in specific brain areas, modulating functions, and pathophysiologies in CNS. Herein, we aimed to evaluate whether activation of CB2R can improve the cognitive impairment in the experimental AD-like model and determine the involved intracellular signaling pathway. Injection of D-galactose (150 mg/kg, i.p.) was performed to urge AD-like features in bilaterally ovariectomized female rats (OVC/D-gal rats) for 8-weeks. Then, AM1241, a CB2R-agonist (3 and 6 mg/kg), was injected intraperitoneally starting from the 6th week. Treatment with AM1241, significantly down-regulated; Toll-like receptor4 (TLR4), Myd88 (TLR4-adaptor protein) genes expression, and the pro-inflammatory cytokines (NFκB p65, TNF-α, IL-6, and IL-12). In contrast, it enhanced BDNF (the brain-derived neurotrophic factor) and CREB (the cyclic AMP response element-binding protein) as well as the immune-modulatory cytokines (IL-4 and IL-10) levels. Moreover, AM1241 lessened the immune-expression of GFAP, CD68, caspase-3, and NFκB p65 markers and mended the histopathological damage observed in OVC/D-gal rats by decreasing the deposition of amyloid plaques and degenerative neuronal lesions, as well as improving their recognition and learning memory in both novel object recognition and Morris water maze tests. In conclusion, activating CB2R by the selective agonist AM1241 can overrun cognitive deficits in OVC/D-gal rats through modulation of TLR4/ NFκB p65 signaling, mediated by modulating CREB/BDNF pathway, thereby can be applied as a potential therapeutic strategy in AD treatment.

Introduction

Alzheimer's disease (AD), the most prevalent form of dementia among older people, is a progressive neurodegenerative disorder marked by cognitive impairment, memory deficits, and behavioral abnormalities [1]. By 2030, AD will affect more than 70 million people worldwide, and this number of patients will grow to be 131 million by 2050 [2]. Accumulation of fibril β-amyloid (Aβ) that forms the extracellular neuritic plaques and intracellular hyperphosphorylated tau protein that forms the intracellular neurofibrillary tangles (NFTs) are the typical histopathological hallmarks of AD [3].

Aβ deposition and tau protein cause synaptic dysfunction, mitochondrial damage, activation of microglia and astrocytes, and eventually leading to neuronal death [4]. In the initial stage of AD, activated microglia and reactive astrocytes protect against neurotoxicity via enhanced phagocytosis of Aβ. The failure to clear Aβ deposits during AD progression contributes to neurodegeneration [5].

Microglia cells, the resident macrophages in the brain, display a quiescent phenotype and transform into an activated state upon chronic deposition of Aβ plaques attempting to clear these aggregates [6]. Previous studies were discretely classified the inflammatory microglial activation states into "M1" and "M2" based on a limited number of cell-surface and secretion markers. However, the clustering of single-cell transcriptomes has shown that the various multifunctional states of microglia do not accurately capture this distinct classification. Moreover, microglia have historically been characterized as "resting," "M1" (pro-inflammatory), or "M2" (anti-inflammatory) based on simple *in vitro* stimulation methods [7, 8]. According to Prinz et al. study [9], advances in imaging and genetics of single-cell technologies provided new insights into the much more complex and fascinating microglia biology. However, the advantage of the "M1/M2" classification is that it gives a simplified nomenclature to distinguish between microglia in functionally distinct states [10].

Further, the M1-like phenotype commonly produces pro-inflammatory cytokines involving TNF-α, IL-6, IL-1β, and highly upregulated surface markers such as CD40, CD86, and CD16/32. Alternatively, the M2-like phenotype produces neurotrophic factors, improving the phagocytosis function and triggering an anti-inflammatory response [11].

The trans-membrane pattern-recognition receptors, Toll-like receptors (TLRs), play a significant role in the innate immune system via identifying various microbes and tissue injury-related ligands [12]. TLRs are stimulated in glial cells (microglia, astrocytes, and oligodendrocytes) and lymphocytes that infiltrate the brain in response to inflammation [13]. Among various TLRs, TLR4 is considered one of the main receptors implicated in the microglial activation via inducing the production of pro-inflammatory cytokines. TLR4 deficit endorses a shift to M2 microglial phenotype, which alleviates the neurodegeneration [14]. Previous research demonstrated that neuroinflammation and other cognitive impairments were ameliorated in TLR4-deficient/knockout mice models [15]. TLR4 induces NF-κB activation via MyD88 dependent and MyD88 independent cascades that lead to the production of pro-inflammatory cytokines [16]. Numerous compounds exhibited therapeutic effect against experimentally induced AD models via inhibiting TLR4 expression, which could suppress the secretion of pro-inflammatory cytokines and subsequent inhibition of microglia activation [17]. To date, only symptomatic therapies for AD are available, and thus there is a necessity for therapies that act on prevention of the disease progression [18].

The endogenous cannabinoid system has emerged as an important pharmacological target for treating neurodegenerative diseases [19]. Cannabinoids are the major constituents of marijuana, and many of the wide spectra of central and peripheral actions of cannabinoids are exerted via two specific cannabinoid receptors, cannabinoid receptors 1 (CB1R) and 2 (CB2R)

[20]. CB2Rs are primarily expressed in immune cells, such as monocytes/macrophages, leukocytes, and lymphocytes [21]. Activation of CB2R has been proved to decrease inflammation and its associated tissue injury via immunosuppressive effects in many pathological disorders, including those associated with neuroinflammation and neurodegeneration [22]. CB2R, as a therapeutic target, plays an important role in the modulation of neuroinflammation and attenuation of activated microglia and astrocytes [23]. Accordingly, there is a need for more effective treatments of AD by using CB2R agonists.

In AD postmortem brains, CB2R was highly expressed, and its role in reducing pro-inflammatory mediators has been proved [24]. Major attention has been given to the therapeutic efficacy of using CB2R specific agonists due to the absence of their psychoactive properties. AM1241, a potent and selective CB2R agonist is one of the most commonly used in research to induce CB2R activation [25].

As cannabinoids exert neuroprotective effects in numerous model systems, our research aimed to explore the probable protective effect of the CB2R agonist, AM1241, in weakening the cognitive and learning deficits in an established AD-like model induced in female rats bilaterally ovariectomized and chronically injected with D-gal. In addition, to determine the signaling cascades underlying that protective effect which prevents AD-like pathological alterations.

Materials and methods

Chemicals

AM1241, (Abcam, ab120934, United Kingdom), was prepared by dissolving 10 mg in 1mL DMSO (Sigma-Aldrich, USA, 03310) (Drug-DMSO), then the drug was freshly prepared daily, by diluting one part of the previous Drug-DMSO mixture in double parts of PBS and intraperitoneally (i.p) injected at 3 and 6 mg/kg b.wt [26]. D-galactose (Sigma-Aldrich G0750, USA) was freshly prepared in 0.9% saline.

Animals

Eighty adult female Sprague-Dawley rats (250–280 g) were utilized in the current study. They were obtained from the National Cancer Institute, Cairo, Egypt. Rats were maintained in the lab under suitable environmental conditions of; temperature (25 ± 2°C), humidity (60%), and good ventilation. Rats were allowed free access to water and normal food pellets. They were left for acclimatization on lab conditions for one week prior to induction of any experimental procedures.

Ethical statement

The experimental design and all animal handling protocols mentioned in the current research were assented by the Institutional Animal Care and Use Committee at Cairo University (CU/II / F / 12 / 19). Efforts were carried out to lessen the suffering of the animals.

Experimental design

Animals were specified into four groups (20 each) at random. Group 1; sham-operated group; at which rats were intraperitoneally (i.p.) injected with saline solution. Group 2 (OVC/D-gal group); rats were subjected to bilateral surgical ovariectomy (OVC), and i.p injected with D-galactose (D-gal) (150 mg/kg) starting one-week post ovariectomy and continued for eight weeks to induce pathological features of Alzheimer's disease, according to the method adopted by **Kamel et al.**, [27]. Groups 3 and 4 (OVC/D-gal+AM1241 groups); rats were subjected to

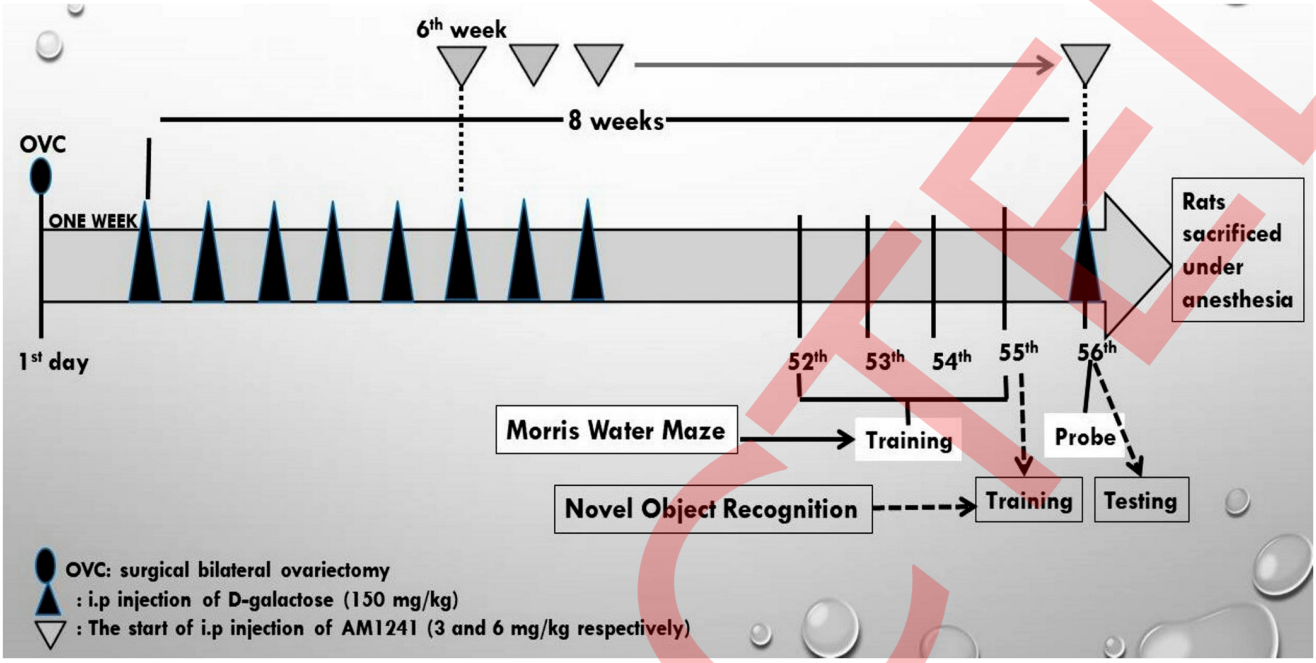

Fig 1. The schematic presentation of the experimental design.

https://doi.org/10.1371/journal.pone.0265961.g001

OVC and D-gal injection as in group 2, then starting from the 6th week, they received i.p injection of 3 and 6 mg/kg respectively of AM1241 [26], concurrently with the D-gal till the end of the experiment.

Prior to the termination of the experiment by five days, rats were submitted to 2 behavioral memory tests, Morris Water Maze (MWM) and Novel Object Recognition (NOR) tests. For NOR, rats were trained on day 55 and tested on day 56. Additionally, they were practiced for four successive days (days 52–55) on MWM, and then on the 5th day (day 56), they were subjected to the probe test (Fig 1). Rats were allowed to rest for one hour between the NOR and MWM to diminish any physical stress on rats between the two tests. After completing the two tests, rats of each group were allocated into two sets. Then they were sacrificed under anesthesia (i.p injection of a mix of 5 mg/kg xylazine and 40 mg/kg Ketamine) by cervical dislocation. The brain was immediately excised and washed with cold saline. The excised brains from each group were divided into two sets. The brains of the first set (5 animals) were allocated for histopathological and immunohistochemical studies; they were preserved in buffered neutral formalin (10%). At the same time, the hippocampi of the second set (15 animals) were dissected out and were kept frozen at −80˚C for further investigation.

Surgical procedures of ovariectomy [28]

Animals were anesthetized using xylazine (10 mg/kg; i.p.) and ketamine hydrochloride (50 mg/kg; i.p, then they were bilaterally shaved at the area between the last rib and the hip. After shaving, the area was disinfected using ethanol 70%. A small incision was made through the skin and muscles. The ovaries with the fat pads were exposed and taken out, and then a suture knot was performed by a hemostatic clamp around the ovarian blood supply just below the ovaries.

Thereafter, the ovaries and part of the oviduct were removed, and the muscle and skin layers were sutured. The wound was sprayed by a mix of bacitracin and povidone-iodine. The

sham-operated control group was exposed to same previous procedures except for ovariectomy. After surgery, animals were wrapped in a piece of cotton and kept in a heated place for at least two hrs. Rats were also injected intraperitoneally with 0.1 ml diclofenac sodium and 0.1 ml ceftriaxone (100 mg/ml) to promote healing. Rats were fed on a soy-free diet to exclude phytosterols' presence in the diet.

Behavioral tests

Novel object recognition test. NOR test was performed to assess the strength of memory to recognize objects and penchant for novelty. The test apparatus was designed as a wooden dark open box (80 length×50width×60cm height) with similar light intensity at every part. Three phases were allocated in this test; habituation, familiarization, and test phases. Wooden objects as cylinders and cubes (each 7-cm height) were put nearby the arena center, and between trials, all objects and box arena were fully swept with 70% ethanol. During the habituation phase of the test, rats were permitted 10 min to scout the apparatus in the absence of the object; 24 h before the practicing. While in the familiarization phase, each rat was put in the empty box, then 5 min later, two similar objects (either familiar cubes or cylinders) were inserted in the arena center. Following this, rats were left to seek the familiar objectives for 10 min then got back to their cage. After 24 h retention, the test phase was carried out, where the animal was left 3 min in the arena in the presence of one novel (cylinder) and one familiar (cube) object. Exploration was determined only by either sniffing or touching the object with the nose. A discrimination index was calculated by comparing the time taken by the rat to explore the familiar object with that spent in searching the novel one, indicated as the ratio of the overall time taken in seeking both objects. Additionally, a preference index was estimated as the time taken scouting the novel object in the test phase, presented as the ratio of the total time spent scouting both objects [29].

Morris water maze test. MWM was employed to estimate memory deficits and spatial learning in rodents. It depends on forming a maze of a rounded pool (180 cm in diameter and 60 cm height) filled with water to the scale of 35 cm and preserved at 25 ± two ˚C. The pool was sectioned into four quadrants, and then a 9 cm in diameter, movable escape platform was placed in a particular quadrant center. Thereafter, the pool was laid in a room dimly lit with distal fixed visual clues, which availed as navigational sign key for placement of the goal. The test was carried out according to the method described by **Alawdi et al**. [30].

Biochemical analysis

Preparation of brain tissue homogenate for biochemical analysis. The collected hippocampal tissues were homogenized in ice-cold phosphate buffer 10% (w/v) in a homogenizer (MPW-120; Medical Instruments). Then, a cooling centrifuge (2k15; Sigma/Laborzentrifugen) was used to centrifuge the obtained homogenate for 5 min at 4000 rpm. Then, the supernatant was obtained for determining the hippocampal tissue contents of NF-κB-p65, TNF-α, BDNF, the pro-inflammatory cytokines (IL-12 and IL-6) as well as the anti-inflammatory cytokines (IL-10 and IL-4) using ELISA kits (Cusabio Biotech, Germany) following the manufacturer directives. Each sample was assayed for each test in triplicate.

Quantitative real-time PCR (RT qPCR) for determination of TLR4 and Myd88 genes. Quantitative reverse transcription-polymerase chain reaction (RT-PCR) was conducted to detect TLR4 and Myd88 genes expression through the next steps.

According to the manufacturer's recommendations, total RNAs were isolated using TRIzol reagent (Invitrogen, Carlsbad, CA, USA). The NanoDrop 2000c (Germany) was utilized to evaluate the quantity and quality of the isolated RNA. A total of 100 ng of RNA was used in QuantiNova SYBR Green RT-PCR Kit (QIAGEN, Hilden, Germany). The qRT-PCR reactions

Table 1. The forward and reverse primers' oligonucleotide sequences for TLR4 and Myd88 genes.

Target	Primers' sequence (5'- 3')
TLR4	F: 5′-AATCCCTGCATAGAGGTACTTCCTAAT-3′
	R: 5′-CTCAGATCTAGGTTCTTGGTTGAATAAG-3′
Myd88	F: 5′-CAACCAGCAGAAACAGGAGTCT-3′
	R: 5′-ATTGGGGCAGTAGCAGATGAAG-3′
βeta actin	F: 5′-TGTTTGAGACCTTCAACACC-3′
	R: 5′-CGCTCATTGCCGATAGTGAT-3′

https://doi.org/10.1371/journal.pone.0265961.t001

were performed in the Applied Biosystem thermal cycler (Applied Biosystems, Foster City, CA, USA) with its attached software version 3.1 (StepOne™, USA). All represented samples from each group were assayed with three biological replicates. All qPCR reactions were assayed at least in duplicates. The cycle threshold (Ct) data was normalized using βeta actin as a housekeeping gene. Relative gene expression was calculated using the ΔΔCT method. The relative quantitation was calculated according to Applied Bio system software using the Δ Ct = Ct gene test–Ct endogenous control equation.

$$\Delta\Delta Ct = \Delta Ct\ sample1 - \Delta Ct\ calibrator$$

$$RQ = Relative\ quantification = 2^{-\Delta\Delta Ct}$$

The RQ is the fold change compared to the calibrator (untreated sample).

The primers' sets utilized in this study are listed in Table 1.

Histopathological examination. Twenty-four hours after formalin fixation, specimens were subjected to routine washing, dehydration in serial dilutions of ethanol, clearing in xylene, and at last embedding in paraffin. Paraffin blocks were sectioned at 4μm, followed by applying hematoxylin and eosin (H&E) as well as Congo red stains according to the method described by **Suvarna and Layton** [31]. A 4-point scale scoring system (0–3) was employed to determine the observed histopathological lesions' degrees of severity. That scoring system denotes; none, changes < 30% (mild), changes 30–50% (moderate), and severe changes > 50% (severe) alterations, respectively [32]. Three serial slices were examined per animal, and then, depending on the examination of the H&E stained slides, five sections per group were immunohistochemically evaluated.

Immunohistochemistry. Paraffin sections were used to detect the immunohisto-expression of GFAP, CD68, caspase-3, NF-κB p65, and CREB. Paraffin sections of sham-operated and all treated groups were incubated with primary monoclonal antibodies against GFAP, CD68, caspase-3, NFκB p65 and CREB (Abcam, Cambridge, MA, USA, ab7260, ab283654, ab32351, ab16502, and ab31387, respectively) at 37˚C for 60 min at dilutions of (1:200, 1:100, 1:100, 1:150, and 1:200 respectively). The sections were exposed to washing in PBS, followed by their incubation at 37˚C for 60 min with the secondary antibody (Dako, Carpenteria, CA, USA). Sections were incubated with biotinylated horseradish peroxidase H and Avidin DH complex according to Vectastain ABC peroxidase kit (Vector Laboratories Inc., Burlingame, CA, USA). After the second wash in PBS, visualization of the reaction was performed using 3,3′-diaminobenzidine tetrahydrochloride (DAB Substrate Kit, Vector Laboratories Inc., Burlingame, CA, USA). Hematoxylin was used as a counterstaining for all sections, followed by dehydration in alcohol and clearance in xylene, then subjected to light microscopic examination. Quantitative analysis of the immune-reactivity of each marker was evaluated in frontal cortex and hippocampus regions using Image J software NIH, version 1.46a, Bethesda, MD,

USA. Ten randomly chosen high (x 400) microscopic fields were examined in each section and presented as the optical density of the positively stained area. All histopathological assessments were performed by an experienced investigator blinded to sample identity to avoid any bias.

Image J analysis software was used to quantify the immune-reactivity of each marker presented by the optical density of the positively stained (brown) areas in ten randomly chosen high power (x400) microscopic fields. Five fields were from the frontal cortex (layers II-V), and the other five were from the hippocampal area (CA3). Finally, we performed statistical analysis for the obtained data.

Statistical analysis

The gained data were subjected to statistical analysis as the mean ± SE (standard error). GraphPad Prism program compared significance between groups via one-way ANOVA and Tukey's multiple comparison tests. Results were considered to be significant when P values < 0.05. For comparing the frequency of the nonparametric data, the Kruskal Wallis H test was used, followed by the Mann-Whitney *U* test for statistical evaluation of the scoring values of the histopathological lesions. The nonparametric data were presented as median.

Results

CB2R receptors activation by AM1241 mended cognitive function in OVC/D-gal rats in MWM and NOR

In NOR, D-galactose administration to ovariectomized rats in the OVC/D-gal group led to a marked ($P<0.05$) decrease in the discrimination index compared to the sham-operated group (0.3±0.03 versus 0.59±0.03). At the same time, administration of AM1241 brought about a dose-related significant ($P<0.05$) elevation in the discrimination index compared to the OVC/D-gal group (0.66±0.02 and 0.95±0.04). Additionally, the time spent by model rats to scout the novel object was lower than that taken by the control sham-operated rats, reflecting a lower preference index (0.27±0.01versus 0.67±0.037). However, AM1241 administered rats preferred the novel object over the familiar one. They spent longer time to scout it, which elevated the preference index (0.79±0.03 and 1.06±0.05) near to normal particularly with the high dose of AM1241 (Fig 2a and 2b).

In MWM, rats in the OVC/D-gal group exhibited a marked ($P<0.05$) elevation in escape latency within the last two days of practicing (39.08±4.520 versus 11.2±2.148) at day 54 and (39.08±3.520 versus 11.2±2.148) at day 55 in the acquisition phase to nearly five times compared to the control sham-operated group. The administration of AM1241 normalized the values of the time required to attain the hidden platform (Fig 2c) as (10.96±1.41587 and 10.58 ±0.915758) at day 54, and (10.96±1.31587 and 10.38±0.946287) at day 55. While, in the probe test, the OVC/D-gal group exhibited lower crossings (46%) above the platform area, added to that, in the target quadrant, they spent less time (49%) (19.36±0.17 versus 41.46±0.408) when compared to control sets. Whereas AM1241 significantly ($P<0.05$) enhanced memory reservation as was obviously noticed by boosting the crossings by 2.1-fold and settling extra time in the target quadrant inspecting for the platform by 2.6-fold, compared with the OVC/D-gal group (42.48±0.32 and 45.84±0.36) (Fig 2d and 2e).

CB2R activation by AM1241 rectified the inflammatory disruption in ovariectomized and D-galactose administrated rats

Estrogen deprivation as a result of bilateral ovariectomy accompanied with D-galactose administration brought about a significant upsurge in the levels of the pro-inflammatory

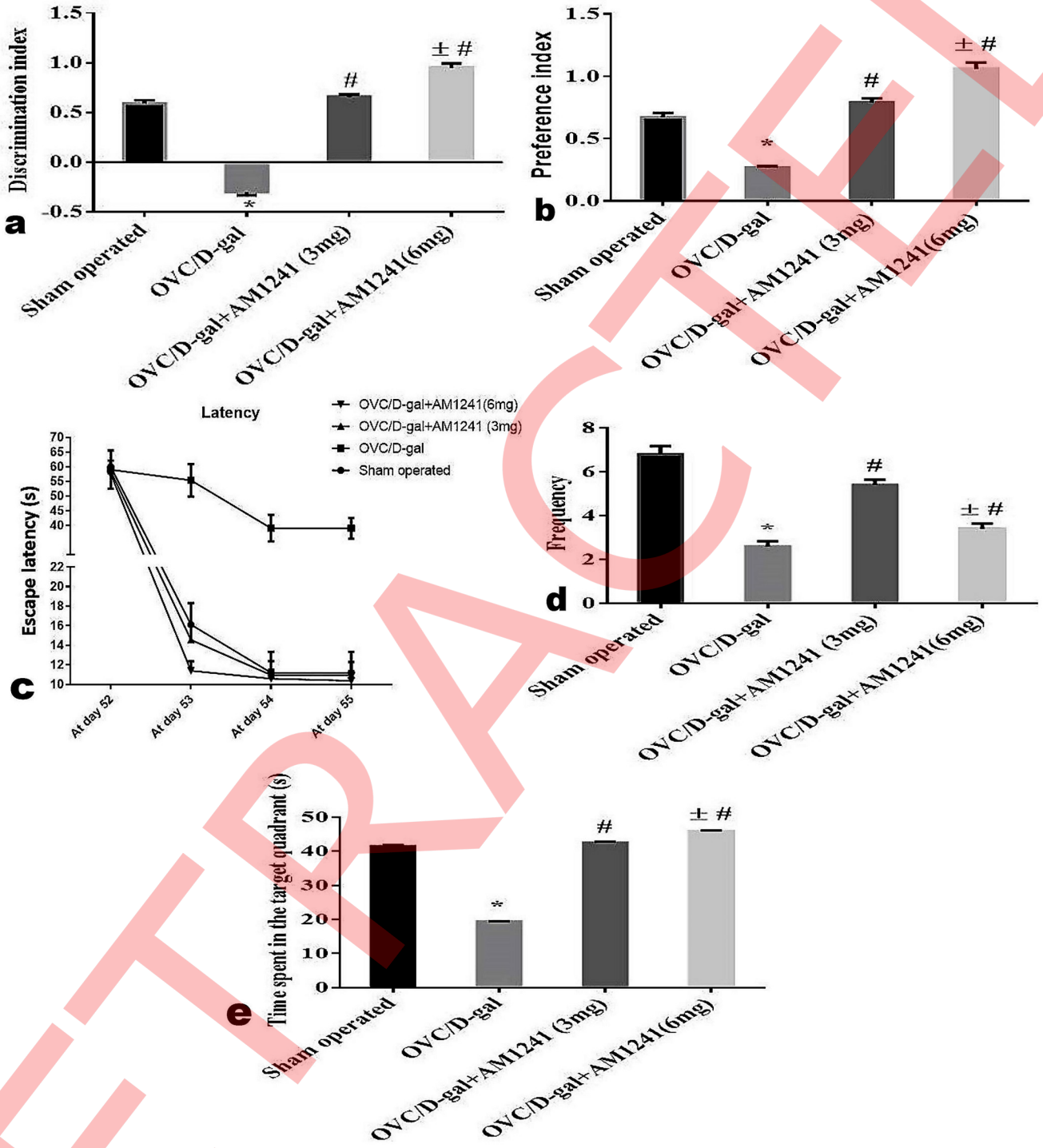

Fig 2. Effect of AM1241 on cognitive functions of OVC/D-gal rats in (a and b) Novel object recognition and (c-e) Morris water maze tests. Data were analyzed by using one way ANOVA followed by Tukey's post hoc test. Values expressed as mean ± SE. *, #, and ± statistically significant different at $P < 0.05$, where; * statistically significant different comparing with control group, # statistically significant different comparing with OVC/D-gal group, ± statistically significant different comparing with AM1241 (3mg/Kg).

https://doi.org/10.1371/journal.pone.0265961.g002

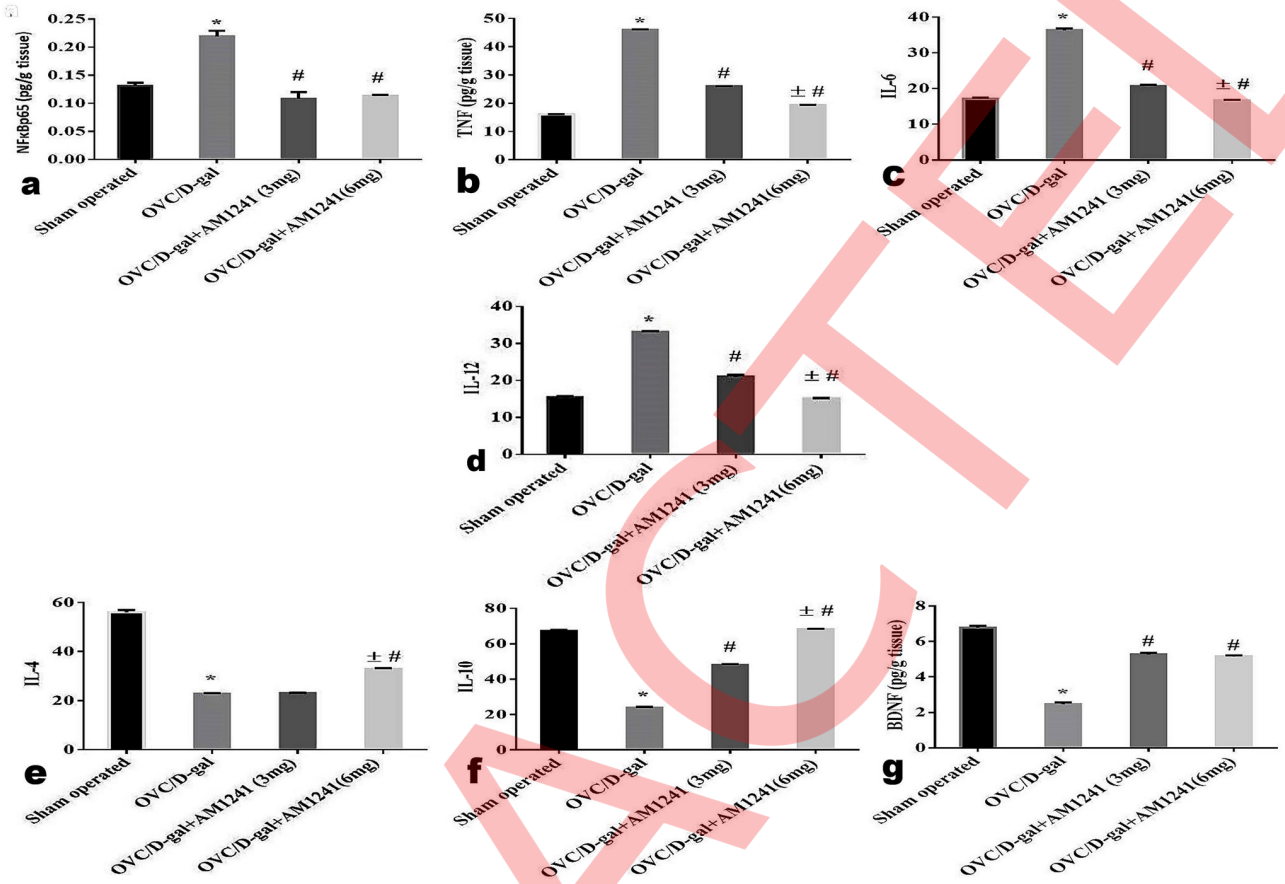

Fig 3. Effect of AM1241 on pro-inflammatory; NFκB p65, TNF-α, IL-6 and IL-12, immune-modulatory; IL-4 and IL-10 levels as well as the neurotrophic factor; BDNF in hippocampal tissue homogenate of OVC/D-gal rats. Data were analyzed by using one way ANOVA followed by Tukey's post hoc test. Values expressed as mean ± SE (n = 15 rats/group). *, #, and ± statistically significant different at $P < 0.05$, where; * statistically significant different comparing with control group, # statistically significant different comparing with OVC/D-gal group, ± statistically significant different comparing with AM1241 (3mg/Kg).

https://doi.org/10.1371/journal.pone.0265961.g003

cytokines encompassing; TNF-α, NFκB p65, IL-6, and IL-12 (46.01±0.19, 0.22±0.01, 36.38 ±0.51 and 33.18±0.28 versus 16±0.141, 0.13±0.006, 17.16±0.347 and 15.48±0.356, respectively) with a significant ($P<0.05$) decrease in the levels of the anti-inflammatory IL-10 and IL-4 cytokines, as well as the neurotrophic protein (BDNF), compared to the sham-operated group. Whilst the levels of the previous pro-inflammatory cytokines were significantly ($P<0.05$) brought down in a dose-related manner with the administration of AM124; TNF-α (26.04 ±0.07 and 19.26±0.195), NFκB p65 (0.11±0.01 and 0.11±00), IL-6 (20.72±0.38 and 16.67 ±0.21), and IL-12 (21.13±0.41 and 15.1±0.22) accompanied with significant ($P<0.05$) elevation in IL-10 (48.13±0.36 and 68.17±0.42), IL-4 (23.06±0.17 and 32.83±0.41), and BDNF (5.27 ±0.09 and 5.15±0.07) levels compared to the OVC/D-gal group, respectively (Fig 3).

AM1241, CB2R agonist restored TLR-4 and Myd88 genes expression in brain tissue of OVC/D-gal group

As presented in Table 2, estrogen deprivation in ovariectomized rats with the administration of D-galactose resulted in a significant ($P<0.05$) increase in the expression of the TLR-4 gene and its adaptor protein, Myd88, compared to the normal sham-operated rats (13.525 ± 0.436

Table 2. The relative TLR4 and Myd88 genes expression in control sham-operated and the other treated groups.

Groups	Sham-operated	OVC/D-gal	OVC/D-gal+AM1241 (3mg/Kg)	OVC/D-gal +AM1241 (6mg/Kg)
TLR4	4.280 ± 0.057	13.525 ± 0.436*	8.642 ± 0.533#	4.835 ± 0.457±#
Myd88	0.956 ± 0.143	1.976 ± 0.436*	1.023± 0. 371#	0.843 ± 0.252±#

Values expressed as mean ± SE. *, #, and ± statistically significantly different at $P < 0.05$, where; * statistically significant difference comparing with the control group, # statistically significant difference comparing with OVC/D-gal group, ± statistically significant difference comparing with AM1241 (3mg/Kg).

https://doi.org/10.1371/journal.pone.0265961.t002

and 1.976 ± 0.436 versus 4.280 ± 0.057 and 0.956 ± 0.143), respectively. Whereas activation of CB2R by i.p injection of AM1241 significantly ($P<0.05$) restored the expression of both TLR-4 (8.642 ± 0.533 and 4.835 ± 0.457) and Myd88 (1.023± 0. 371 and 0.843 ± 0.252) genes compared to their levels in the OVC/D-gal group, particularly with the high dose treatment.

AM1241 administration improved histological alterations induced by D-gal administration in ovariectomized rats

The frontal cortical and hippocampal areas of sham-operated rats showed normal histological structure (Fig 4a–4c). While, brain sections of the OVC/D-gal rats' group, revealed marked tissue alteration in both frontal cortex and hippocampus. The frontal cortex (layers II-V) showed various neuronal degenerative changes particularly, vacuolar degeneration, dark neurons with accentuated dusky cytoplasm, shrunken, and ghost-like neurons (Fig 4d). Neuronophagia was a prominent finding with scattered apoptotic neurons (Fig 4e). Corkscrew appearance (Fig 4f) of the neuronal apical dendrites was a common finding in the cortical neurons with conspicuously observed amyloid plaques of variable sizes (Fig 4g), which stained positively with Congo red stain (Fig 4h) either intraneuronal or as a cerebral amyloid angiopathy in the cerebral blood vessels' walls. Neurofibrillary tangles of the neuronal cell bodies, astrocytes' hyperactivity, and an obvious glial nodules (Fig 4i) were common findings. The dorsal hippocampus showed variable degrees of neuronal degeneration. The dentate gyrus (DG) showed vacuolation and loss of the small pyramidal cells and scattered degenerated cells in the granular layer (Fig 4j). The cornu Ammonis (CA) 1 and 3 subdivisions showed degeneration of their neurons and necrosis of some scattered ones with an obvious presence of different sizes amyloid plaques, which stained positively with Congo red stain (Fig 4k and 4l). On the contrary, the co-administration of AM1241 (3 and 6mg/kg) at the 6th week from D-gal administration in OVC/D-gal rats showed a dose-related reversion of the ongoing appearance of the hallmarks lesions of Alzheimer's disease-like. The cerebral cortex showed scarce neuronal cells degeneration (Fig 5a, 5b, 5e and 5f) with or without rare appearance of amyloid plaques. The hippocampi of those rats showed an absence of the amyloid plaques, degenerative changes of mild degree of the pyramidal cells of the DG area, sparse pyknotic neurons, and neuronophagia in the molecular layer (Fig 5c, 5d, 5g and 5h). The observed histopathological lesions were summarized and scored in (Fig 5i).

Effect of AM1241 administration on the immune-expression of; GFAP, CD68, caspase-3, NFκB p65 and the neuroplastic marker, CREB in OVC/D-gal rats

Brain sections of control sham-operated rats revealed normal few scattered CD68 positive microglia cells (Fig 6a and 6b) as well as few GFAP positive astrocytes of small-size and few short processes (Fig 6c and 6d), negative expression of both caspase-3 (Fig 7a and 7b) and NFκB p65 (Fig 7c and 7d) as well as marked expression of CREB (Fig 8a and 8b) in both

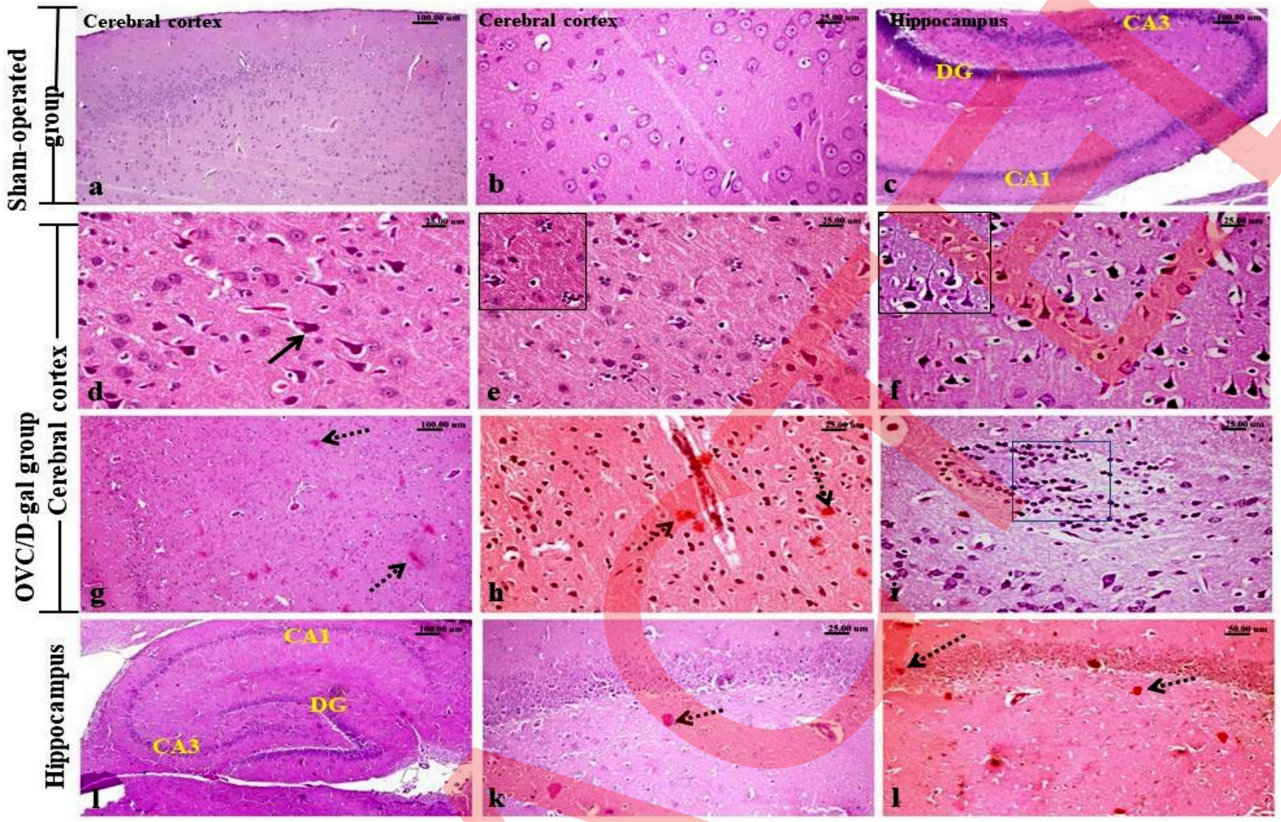

Fig 4. H&E stained photomicrographs of frontal cortex and hippocampus, (a-c) Sham-operated group, showing normal histological structure. (d-l) OVC/D-gal group, showing; (d) neuronal cells degenerative changes as shrunken neurons with accentuated dusky cytoplasm, vacuolar degeneration (e) marked neuronophagia (upper corner) with scattered apoptosis, (f) corkscrew appearance of the neuronal apical dendrites (g) variable sizes amyloid plaques (dotted-arrow) which (h) stained positively with Congo red stain, (i) glial nodules with satellatosis around degenerated neuron. (j-l) dorsal hippocampus showing vacuolation and loss of the small pyramidal cells of the dentate gyrus (DG) with degenerated cells in the granular layer as well as in Cornu Ammonis (CA) 1 and 3 subdivisions with (k) different sizes amyloid plaques (dotted-arrow) which (l) stained positively with Congo red stain. Fig 4C is excluded from this article's CC BY license. See the accompanying retraction notice for more information.

https://doi.org/10.1371/journal.pone.0265961.g004

frontal cortex and hippocampal areas. While brain sections of the OVC/D-gal rats' group showed more activation of microglial and astrocytes betokened by increased immune-reactive CD68 cells (1.8±0.05, versus 0.44±0.051) (Fig 6e and 6f), and widespread positive GFAP astrocytes (3.75±0.11 versus 1.28±0.066) with multiple elongated processes (Fig 6g and 6h), increased expression of both caspase-3 (1.78±0.13 versus 0.07±0.028) (Fig 7e and 7f), and NFκB p65 (4.39±0.10 versus 0.05±0.022) (Fig 7g and 7h) as well as decreased expression of CREB (1.44±0.09 versus 4.96±0.068) (Fig 8c and 8d). The co-administration of AM1241 with D-galactose for 3weeks to ovariectomized rats markedly decreased the immune-reactivity of CD68 (0.98±0.09 and 0.67±0.06) (Fig 6i, 6j, 6m and 6n), GFAP (2.26±0.1 and 1.66±0.09) (Fig 6k, 6l, 6o and 6p), caspase-3 (0.7±0.04 and 0.54±0.02) (Fig 7i, 7j, 7m and 7n), and NFκB p65 (2.56±0.05 and 1.59±0.07) (Fig 7k, 7l, 7o and 7p) with the boosted expression of CREB (2.92 ±0.07 and 4.11±0.06) (Fig 8e–8h) in a dose-related response as confirmed by quantification of all markers' positive expression by the image analysis software.

Discussion

Away from the traditional strategies in treating AD, the current study investigated the role of activating CB2R using the synthetic agonist; AM1241 in mitigating cognitive dysfunction and

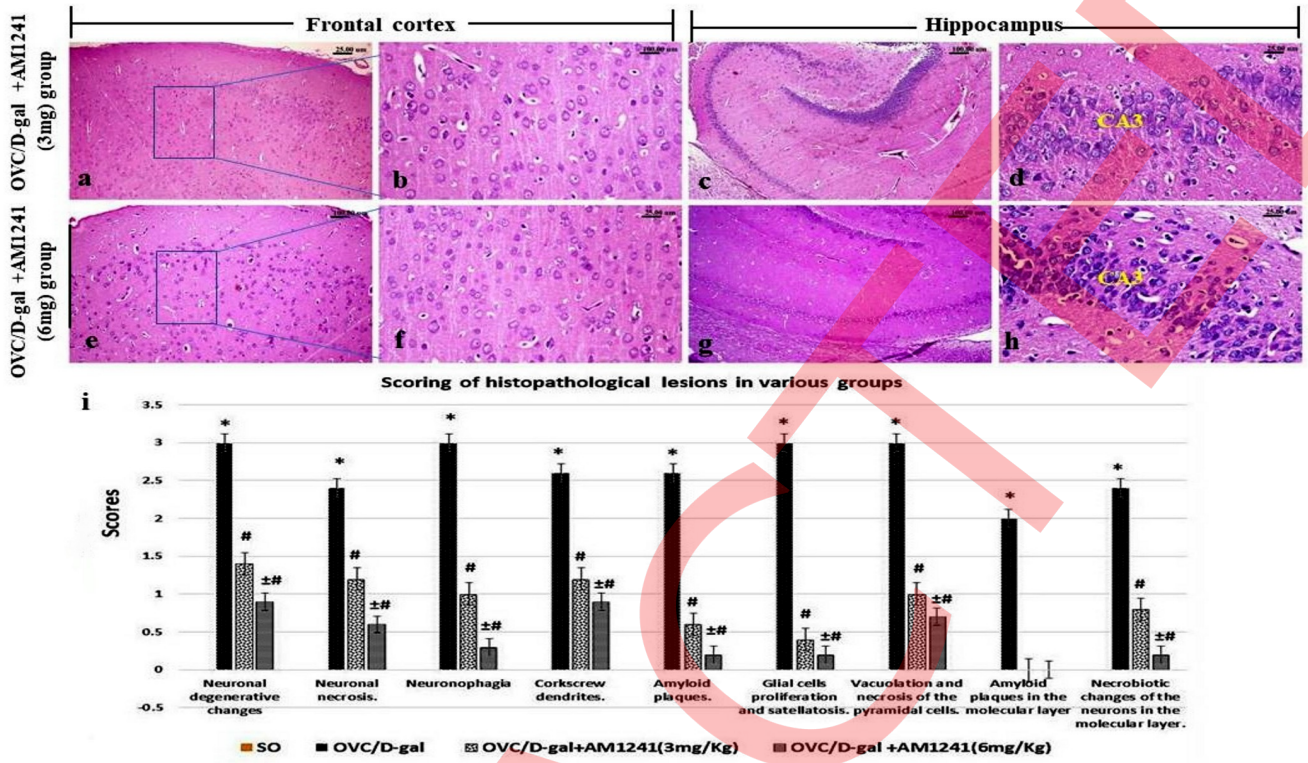

Fig 5. H&E stained photomicrographs of frontal cortex and hippocampus areas of AD-model rats which treated with AM1241, (a-d) 3mg/kg and (e-h) 6mg/kg showing; few cerebral cortical scattered degenerated and necrotic neurons, absence of amyloid plaques with hippocampal disappearance of the amyloid plaques, mild degenerative changes of the DG and CA neurons. (i) The scoring of the observed histopathological lesions in various groups (Data are presented as median (n = 5 rats/group) using Kruskel-Wallis test followed the Mann-Whitney *U* test. Significantly different was considered at $P<0.05$, where; * significantly different when compared to control group, # significantly different when compared to OVC/D-gal group, ± significantly different when compared to AM1241 (3mg/Kg). Figs 5B-D and G-H are excluded from this article's CC BY license. See the accompanying retraction notice for more information.

https://doi.org/10.1371/journal.pone.0265961.g005

AD-like pathological changes. Our findings support the restoration of the cognitive function and attenuation of the progression of AD-like pathological alterations induced by D-galactose injections in ovariectomized female rats through activation of CB2R, presenting it as a novel therapeutic target for neurodegenerative diseases, particularly AD.

To achieve our aim, our model for AD-like depended on induction of ovariectomy of female rats followed by intraperitoneal injection of D-gal at a dose of 150 mg/kg/day for eight weeks to stimulate AD-like associated pathologies as well as cognition impairment. Ovariectomy (OVC), a widely used model of menopause, has been reported to impair the learning and memory capacity of female rats, induce neuroinflammation, and reduce neurotrophic factor levels. Estrogen depletion (induced by bilateral ovariectomy of female rats) substantially contributes to memory loss and cognitive decline, ensuring AD-like pathology. Additionally, estrogen deficiency was mentioned to play the main role in initiating and progressing neurodegenerative disorders [33]. Moreover, estrogen deprivation has been shown to cause Aβ deposition, neurofibrillary tangle formation, and spatial memory impairment in ovariectomized rats [34]. D-gal is an aging agent that disrupts memory and synaptic function through inflammatory progression. It was confirmed that D-gal at high doses bounded with the free amino groups of proteins to produce advanced glycation endproducts (AGEs) inducing oxidative stress. Its administration in rodents causes neurobehavioral changes containing cognition and motor impairment, diminished neurogenesis, neurodegeneration, caspase-dependent apoptosis, and mitochondrial

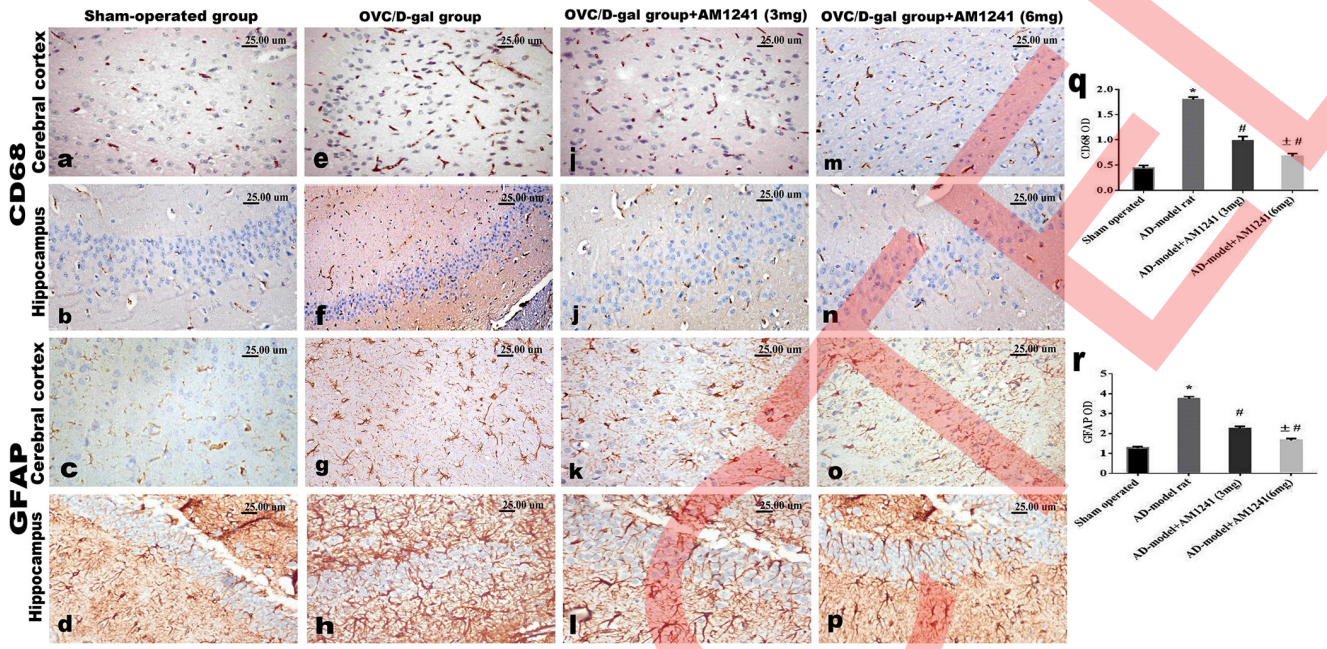

Fig 6. Photomicrographs of CD68 and GFAP immune-stained sections of frontal cortex and hippocampus. (a-d) Sham-operated group showing normal few scattered CD68 positive microglia cells and few scattered small sized GFAP positive astrocytes. (e-h) OVC/D-gal group showing intense expression of both markers denoting hyper-activation of microglia and astrocyte cells. OVC/D-gal rats' which treated with AM1241, (i-l) 3mg/kg and (m-p) 6mg/kg showing a dose related decreased the immuno-reactivity of CD68 and GFAP. (q and r) image analysis software for quantification of the positive expression of both CD68 and GFAP (data were analyzed by using one way ANOVA followed by Tukey's post hoc test. Values expressed as mean ± SE (n = 5 rats/group). *, #, and ± statistically significant different at $P < 0.05$, where; * statistically significant different comparing with control group, # statistically significant different comparing with OVC/D-gal group, ± statistically significant different comparing with AM1241 (3mg/Kg). Figs 6D and K-L are excluded from this article's CC-BY license. See the accompanying retraction notice for more information.

https://doi.org/10.1371/journal.pone.0265961.g006

dysfunction [35]. Some studies allocated D-gal-sham group in their experimental design along with OVC/D-gal group to explore the ideal AD-like rodent model such as **Hua X et al** [36]. They found that the typical histopathological alterations associated with AD were observed in the hippocampi of OVC rats injected with D-gal but not in other control groups and these two components act synergistically to accelerate the pathophysiological course of AD. Thus, long-term OVX combined with D-gal injection serves as an ideal AD rodent model capable of mimicking pathological, neurochemical and behavioral alterations in AD.

Moreover, other previous studies as Kamel et al [27] have indicated that estrogen deprivation and D-gal administration act synergistically to accelerate the pathophysiological course of AD. Therefore, OVC along with D-gal injection represents a perfect AD-like experimental model to mimic the behavioral, neurochemical, and pathological alterations in AD.

In the current work, the findings of the Morris water maze (MWM) test and the novel object recognition test (NOR) exhibited that; OVC/D-gal rats revealed impaired both spatial and recognition memories, these observations are in accordance with those of other studies [36, 37]. At the same time, treatment with CB2R agonist (AM1241) after D-galactose injection to ovariectomized rats could alleviate spatial and recognition memory impairments. The latter alleviation could be eventuated via mitigating mechanisms implicated in the release of pro-inflammatory cytokines via TLR4 signaling, which was confirmed by the observed alleviation in the neuroinflammatory cytokines, including IL-6, IL-12, and TNF-α. These data are matching with those of **Martín-Moreno et al**. [38], who confirmed that activation of CB2R via synthetic or endogenous CB2R agonists has shown a neuroprotective effect via reducing

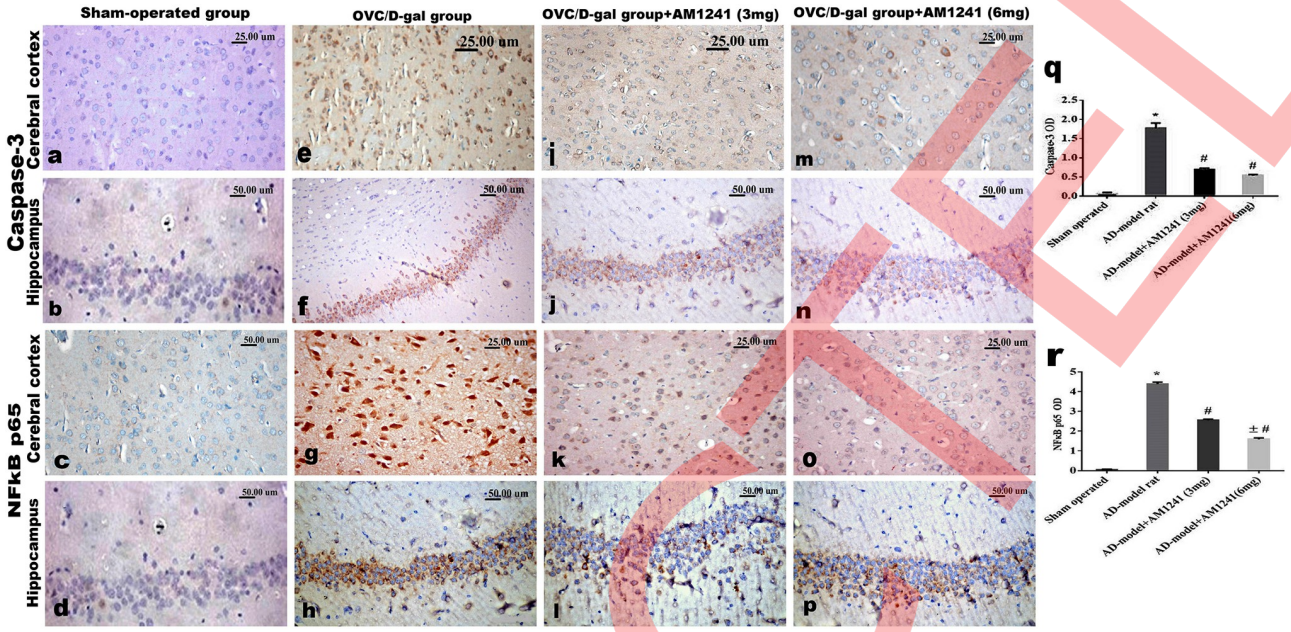

Fig 7. Photomicrographs of caspase-3 and NFκB p65 immune-stained sections of frontal cortex and hippocampus. (a-d) Sham-operated group showing negative expression of caspase-3 and NFκB p65. (e-h) OVC/D-gal group showing intense expression of caspase-3 and NFκB p65 among the neuronal cells. AD-model rats' which treated with AM1241, (i-l) 3mg/kg and (m-p) 6mg/kg showing marked decreased expression of caspase-3 and NFκB p65 in a dose related response. (q and r) image analysis software for quantification of the positive expression of both caspase-3 and NFκB p65 (data were analyzed by using one way ANOVA followed by Tukey's post hoc test. Values expressed as mean ± SE (n = 5 rats/group). *, #, and ± statistically significant different at $P < 0.05$, where; * statistically significant different comparing with control group, # statistically significant different comparing with OVC/D-gal group, ± statistically significant different comparing with AM1241 (3mg/Kg).

https://doi.org/10.1371/journal.pone.0265961.g007

inflammation in Tg APP transgenic mice (a transgenic amyloid precursor protein (APP) mice).

Microglia activation has two phenotypes, M1 and M2. The classically activated M1 (neurotoxic cells) phenotype produces pro-inflammatory mediators involving IL-1β, TNF-α, IL-6, and CD68. Conversely, the M2 phenotype is characterized by anti-inflammatory properties,

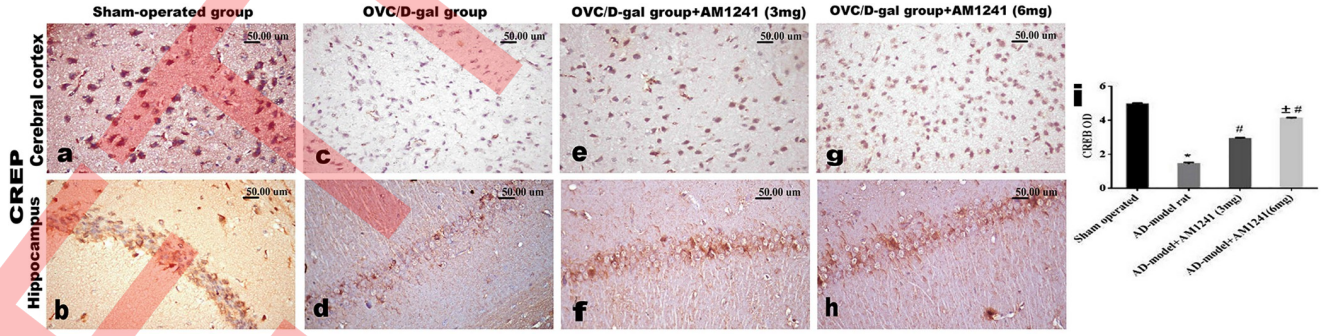

Fig 8. Photomicrographs of CREB immune-stained sections of frontal cortex and hippocampus. (a-b) Sham-operated group showing marked expression of CREB. (c-d) OVC/D-gal group showing diminished CREB expression among the neuronal cells. AD-model rats' which treated with AM1241, (e-f) 3mg/kg and (g-h) 6mg/kg showing restored boosted expression of CREB. (i) Image analysis software for quantification of the positive expression of CREB (data were analyzed by using one way ANOVA followed by Tukey's post hoc test. Values expressed as mean ± SE (n = 5 rats/group). *, #, and ± statistically significant different at $P < 0.05$, where; * statistically significant different comparing with control group, # statistically significant different comparing with OVC/D-gal group, ± statistically significant different comparing with AM1241 (3mg/Kg).

https://doi.org/10.1371/journal.pone.0265961.g008

which have a role in tissue remodeling and repair via the production of IL-4, IL-10, and transforming growth factor (TGF-β1) anti-inflammatory cytokines, as well as neurotrophic factors involving brain-derived neurotrophic factor (BDNF) and glial-derived neurotrophic factor (GDNF) [39, 40].

Activated microglia and astrocytes express TLR4, which in turn activates the NF-κB signaling pathway with the release of pro-inflammatory mediators [41]. Additionally, microglial activation and aggregation are stimulated as a consequence to Aβ deposition via TLR4 signaling, enhancing phagocytosis and cytokine production [42]. Upon TLR4 activation, it stimulates the activation of transcriptional factor NF-κB that is required for the expression of many pro-inflammatory mediators, including TNF-α, interleukin-1β (IL-1β), and interleukin-6 (IL-6). The overexpression of these pro-inflammatory cytokines further induces microglial activation, producing a cycle of neuroinflammation [43].

Our results showed a significant upregulation of TLR4 expression and its downstream target NF-κB-P65 in the OVC/D-gal group. Moreover, the pro-inflammatory cytokines TNF-α, IL-6, and IL-12 were markedly upregulated in the OVC/D-gal group, which the activation of the TLR-4/p65-NF-κB pathway can partially explain. Concomitantly, the anti-inflammatory cytokines, IL-4, and IL-10 expression were significantly declined in the OVC/D-gal group. Parallel with our findings, **Xia et al**. [44] clarified that D-gal byproduct, AGE (advanced glycation end-products), binds with the AGE receptor (RAGE) and/or TLR4 to induce inflammatory responses (cytokines production). These results further support the role of TLR4 in neuroinflammation in OVC/D-gal rats. Our data are compatible with prior findings of **Bierhaus et al**. [45] **and Srikanth et al**. [46] who observed that D-gal could activate NF-κB and elevated the production of pro-inflammatory mediators such as TNF-α, RAGE over-expression. Additionally, D-gal could booste both ROS and TLR4 expression levels, which further activated NF-κB and its downstream inflammatory cascades as well as activated both astrocytes and microglia cells. Over and above, our current results revealed that the activation of CB2R via AM1241 mitigated the elevations in TLR4 expression and its downstream effector NF-κB-P65.

Moreover, the CB2R agonist markedly inhibited the expression of the pro-inflammatory cytokines TNF-α, IL-6, and IL-12, whereas those of the anti-inflammatory properties (IL-4 and IL-10) were significantly elevated. The later findings agree with those of **Adhikary et al**. [47], who showed that pharmacological activation of CB2R inhibited TLR4 expression after spinal cord injury. In agreement, CB2R activation was reported to attenuate acute liver failure induced by D-galactose/lipopolysaccharide (LPS) via shifting the M1 to M2 state of macrophages and by stimulating the TLR4 expression as well. Therefore, our results displayed that CB2R activation could suppress both cognitive and motor impairments after suppressing neuroinflammation via a significant decrease in the M1 phenotype and the pro-inflammatory cytokines (TNF-α, IL-6, and IL-12). As well as an increase in M2 and anti-inflammatory cytokines (IL-4 and IL-10) expression through inhibiting the TLR-4/p65-NF-κB signaling pathway. All of the later observations were supported by our histopathological findings, including stoppage of the progress of Alzheimer's disease-like hallmark lesions, such as; mild degenerative changes and the rare appearance of amyloid plaques and neurofibrillary tangles. The latter coincided with the observation of **Aso et al**., [48] who stated that AD treatment with CB2R agonists was proved to promote the amyloid senile plaques clearance and the recovery of the neuronal synaptic plasticity in animal models. Moreover, the activation of the CB2R led to suppression of neuroinflammatory pathways and restoration of activated microglia from pro-inflammatory to anti-inflammatory state [49].

Further, chronic administration of D-galactose can cause ROS generation and excessive free radicals' production, contributing to apoptosis through the release of several apoptogenic

factors. Caspase-3 is involved in regulating microglia activation, and the impairment of its activation was proved to protect against neuronal loss in numerous brain diseases experimental models [49]. In our study, significant increased expression of caspase-3 was observed in the OVC/D-gal group, which agrees with the finding of **Du et al**. [50]. According to a previous study, D-gal stimulates ROS generation that results in the activation of c-Jun NH2-terminal kinase (JNK) and the release of cytochrome c from mitochondria into the cytosol further stimulates the activation of caspase-3 and the initiation of apoptosis [51]. Meantime, activation of CB2R by the agonist administration significantly increased cellular viability by inactivating caspase-3, a result which is in accordance with **Jeong et al**., [52], who stated that CB2R agonist could protect against apoptosis via blocking the activation of a series of caspases, including caspase-3. Additionally, **Viscomi et al**. [53] revealed that CB2R activation could counteract apoptotic cell death by regulating JNK phosphorylation through PI3K/Akt signaling pathway.

The current work investigated whether CB2R activation via AM1241 treatment exerts a protective effect on OVC/D-gal rats' via modulation of the CREB/BDNF signaling pathway. The CAMP-responsive element-binding protein (CREB) has been known as a key element for learning, memory, and neuronal plasticity. CREB phosphorylation was found to be reduced in AD patients and experimental AD-like models. Activation of CREB in neurons has been associated with several intracellular processes, including neurogenesis and neuronal plasticity [54]. Phosphorylation of CREB enhances the expression of various pro-survival genes as Bcl-2 and BDNF and promotes the expression of both antioxidant enzymes and the antiapoptotic proteins, as well as reduces the delayed neuronal death [55]. CREB was mentioned to regulate the transcription of its target gene, brain-derived neurotrophic factor (BDNF). However, the synaptic function and activation of CREB were linked to the elevation in BDNF secretion [56]. The most abundant neurotrophic factor in the hippocampus, BDNF, plays a vital role in neuronal survival and synaptic plasticity by preventing neuronal injury and increasing neurogenesis as well as cell survival.

Over and above, BDNF binds to its receptor, tyrosine receptor kinase B (Trk-B), which stimulates the phosphorylation and activation of transcription factors such as CREB, which stimulates gene expression [57]. In brain, BDNF is expressed by glial cells, such as astrocytes and microglia [58], and the downregulation of BDNF is implicated in the pathogenesis of neurodegenerative diseases. The present data revealed the ability of the CB2R agonist to restore the expression of CREB and BDNF levels in OVC/D-gal rats, proposing that the antioxidant efficacy of CB2R agonist plays a role in its neuroprotective effect. Consistent with our results, cannabinoids have been proved to stimulate CREB phosphorylation and enhance changes in BDNF and CREB genes expression [59]. In addition, it has been demonstrated that endocannabinoids stimulate phosphorylation of the BDNF receptor (Trk-B) via activating MAP kinase/ERK kinase pathways [60]. Our findings align with that of **Choi et al**. [61] who revealed that the cortical CB2R activation ameliorated cerebral ischemic injury potentially through modulation of CREB/ BDNF signaling pathway. These findings together exposed that the elevation in the CREB/ BDNF pathway expression via CB2R agonist treatment could mitigate AD-like pathologies in OVC/D-gal rats.

On the other side, astrocyte is the most abundant brain glial cell type that plays several vital functions, including modification of synapse signaling, metabolic support of neurons, and recycling of neurotransmitters. Upon activation, astrocytes transformed to an inflammatory state, and this process is termed reactive astrogliosis. Reactive astrocytes are stimulated by some pathological disorders in the microenvironment surrounding the astrocytes, as the aggregation of Aβ plaques [62]. Reactive astrocytes are phagocytic cells capable of engulfing Aβ aggregates, especially in the early stages of Alzheimer's disease [63]. Reactive astrogliosis is characterized by increased expression of GFAP, and the degree of astrogliosis is associated with the degree of cognitive decline [64]. In the current study, OVC/D-gal induced a

significant degree of astrogliosis marked by increased GFAP expression. The oxidative stress-induced in our AD-like model via ovariectomy and D-gal injections is proposed to stimulate astrocytes to switch from a resting to a reactive phenotype. This suggestion is consistent with a previous study, which showed the elevation of ROS induced astrocyte injury and consequently increased the glial fibrillary acidic protein (GFAP) expression in the brain [65]. Our results revealed that CB2R activation could suppress astrogliosis, as evidenced by downregulation of GFAP expression. Consistent with our results, **Avraham et al**. [25] observed a significant decrease in astrogliosis and gliogenesis in GFAP/Gp120 transgenic mice following the administration of CB2R agonist, AM1241, which diminished the immunofluorescence of GFAP expression that supports the anti-inflammatory action of the CB2 receptors. In our OVC/D-gal group, elevated expression of CD68+ was observed. In the same line, activated microglia cells express numerous surface markers in response to damage, such as CD68, a microglial activation marker that is readily expressed in its endolysosome and the plasma membrane. There is a strong association between CD68 and poor cognitive function, dementia, and tau pathology (i.e., neuritic plaques and tangles). Elevated expression of CD68+ microglia is associated with neurodegenerative diseases [66]. In our current work, we observed that the activation of CB2R by AM1241 reversed the elevation of CD68 expression. Consistently, a previous study by **Gómez-Gálvez et al**. [67] demonstrated that CB2R activation normalized the elevated expression of CD68 in Parkinson's disease.

In conclusion, our current study revealed that the TLR4/NF-κB signaling pathway participates in the pathogenesis of AD-like features promoting the inflammatory cascade. CB2R activation using their agonist, AM1241 could exert a neuroprotective effect via suppressing the activation of TLR4/NF-κB p65 inflammatory signaling through curbing its adaptor protein (Myd88) and augmenting the associated CREB/BDNF expression in brain tissues. Additionally, CB2R activation could lessen astrocytes and microglial activation as well as apoptosis. Our results reinforced the assumption that the activation of CB2R could be regarded as a potential target for the novel therapeutic approaches against AD.

Supporting information

S1 Data.
(XLSX)

Author Contributions

Conceptualization: Sahar S. Abd El-Rahman.

Data curation: Sahar S. Abd El-Rahman.

Methodology: Sahar S. Abd El-Rahman, Hany M. Fayed.

Software: Hany M. Fayed.

Writing – original draft: Sahar S. Abd El-Rahman, Hany M. Fayed.

Writing – review & editing: Sahar S. Abd El-Rahman, Hany M. Fayed.

References

1. DeTure MA, Dickson DW The neuropathological diagnosis of Alzheimer's disease. Mol Neurodegener. 2019; 14(1): 32. https://doi.org/10.1186/s13024-019-0333-5 PMID: 31375134
2. Yang P, Guo Y, Sun Y, Yu B, Zhang H, et al. Active immunization with norovirus P particle-based amyloid-beta chimeric protein vaccine induces high titers of anti-Abeta antibodies in mice. BMC Immunol. 2019; 20: 9. https://doi.org/10.1186/s12865-019-0289-9 PMID: 30755174

3. Ittner LM, Gotz J Amyloid-beta and tau—a toxic pas de deux in Alzheimer's disease. Nat Rev Neurosci. 2011; 12: 65–72. https://doi.org/10.1038/nrn2967 PMID: 21193853

4. Takahashi R, Nagao T, Gouras G Plaque formation and the intraneuronal accumulation of β-amyloid in Alzheimer's disease: Intraneuronal accumulation of β-amyloid. Pathol Int. 2017; 67(4):185–193. https://doi.org/10.1111/pin.12520 PMID: 28261941

5. Gambuzza M, Sofo V, Salmeri F, Soraci L, Marinoc S, et al. Toll-Like Receptors in Alzheimer's Disease: A Therapeutic Perspective. CNS Neurol Disord Drug Targets. 2014; 13(9):1542–58. https://doi.org/10.2174/1871527313666140806124850 PMID: 25106635

6. Tejera D, Mercan D, Sanchez-Caro JM, Hanan M, Greenberg D, et al. Systemic inflammation impairs microglial Aβ clearance through NLRP3 inflammasome. The EMBO j. 2019; 38: e101064–e101064. https://doi.org/10.15252/embj.2018101064 PMID: 31359456

7. Martinez FO, Gordon S The M1 and M2 paradigm of macrophage activation: time for reassessment. F1000Prime Rep. 2014; 6: 13 https://doi.org/10.12703/P6-13 PMID: 24669294

8. Ransohoff RM A polarizing question: do M1 and M2 microglia exist? Nat Neurosci. 2016; 19: 987–991 https://doi.org/10.1038/nn.4338 PMID: 27459405

9. Prinz M, Jung S, Priller J Microglia Biology: One Century of Evolving Concepts. Cell. 2019; 179: 292–311. https://doi.org/10.1016/j.cell.2019.08.053 PMID: 31585077

10. Benusa SD, George NM, Dupree JL Microglial heterogeneity: distinct cell types or differential functional adaptation? Neuroimmunology and Neuroinflammation. 2020; 7: 248–263.

11. Orihuela R, McPherson CA, Harry GJ Microglial M1/M2 polarization and metabolic states. Br. J. Pharmacol. 2016; 173: 649–665. https://doi.org/10.1111/bph.13139 PMID: 25800044

12. Calvo-Rodriguez M, García-Rodríguez C, Villalobos C, Núñez L Role of Toll Like Receptor 4 in Alzheimer's Disease. Front Immunol. 2020; 11: 1588. https://doi.org/10.3389/fimmu.2020.01588 PMID: 32983082

13. Okun E, Griffioen K, Lathia J, Tang S-C, Mattson M, et al. Toll-Like Receptors in Neurodegeneration. Brain Res Rev. 2008; 59: 278–292. https://doi.org/10.1016/j.brainresrev.2008.09.001 PMID: 18822314

14. Miron J, Picard C, Frappier J, Dea D, Théroux L, et al. TLR4 Gene Expression and Pro-Inflammatory Cytokines in Alzheimer's Disease and Response to Hippocampal Deafferentation in Rodents. J Alzheimers Dis. 2018; 63: 1547–1556. https://doi.org/10.3233/JAD-171160 PMID: 29782315

15. Muhammad T, Ikram M, Ullah R, Rehman SU, Kim MO Hesperetin, a Citrus Flavonoid, Attenuates LPS-Induced Neuroinflammation, Apoptosis and Memory Impairments by Modulating TLR4/NF-κB Signaling. Nutrients. 2019; 11(3):648.

16. Du Y, Qian B, Gao L, Tan P, Chen H, et al. Aloin Preconditioning Attenuates Hepatic Ischemia/Reperfusion Injury via Inhibiting TLR4/MyD88/NF-κB Signal Pathway In Vivo and In Vitro. Oxid Med Cell Longev. 2019; 11:1–14. https://doi.org/10.1155/2019/3765898 PMID: 31827674

17. Paudel YN, Angelopoulou E, Piperi C, Othman I, Aamir K, et al. Impact of HMGB1, RAGE, and TLR4 in Alzheimer's Disease (AD): From Risk Factors to Therapeutic Targeting. Cells. 2020; 9: 383.

18. Velazquez R, Ferreira E, Knowles S, Fux C, Rodin A, et al. Lifelong choline supplementation ameliorates Alzheimer's disease pathology and associated cognitive deficits by attenuating microglia activation. Aging Cell. 2019; 18: e13037. https://doi.org/10.1111/acel.13037 PMID: 31560162

19. Fernández-Ruiz J, Romero J, Ramos JA Endocannabinoids and Neurodegenerative Disorders: Parkinson's Disease, Huntington's Chorea, Alzheimer's Disease, and Others. Handb Exp Pharmacol. 2015; 231: 233–259. https://doi.org/10.1007/978-3-319-20825-1_8 PMID: 26408163

20. Piomelli D The molecular logic of endocannabinoid signalling. Nat Rev Neurosci. 2003; 4: 873–884. https://doi.org/10.1038/nrn1247 PMID: 14595399

21. Howlett AC, Barth F, Bonner TI, Cabral G, Casellas P, et al. International Union of Pharmacology. XXVII. Classification of cannabinoid receptors. Pharmacol Rev. 2002; 54: 161–202. https://doi.org/10.1124/pr.54.2.161 PMID: 12037135

22. Pacher P, Mechoulam R Is lipid signaling through cannabinoid 2 receptors part of a protective system? Prog Lipid Res. 2011; 50: 193–211. https://doi.org/10.1016/j.plipres.2011.01.001 PMID: 21295074

23. Concannon RM, Okine BN, Finn DP, Dowd E Differential upregulation of the cannabinoid CB(2) receptor in neurotoxic and inflammation-driven rat models of Parkinson's disease. Exp Neurol. 2015; 269: 133–141. https://doi.org/10.1016/j.expneurol.2015.04.007 PMID: 25895887

24. Benito C, Tolón RM, Pazos MR, Núñez E, Castillo AI, et al. Cannabinoid CB2 receptors in human brain inflammation. Br J Pharmacol. 2008; 153: 277–285. https://doi.org/10.1038/sj.bjp.0707505 PMID: 17934510

25. Avraham HK, Jiang S, Fu Y, Rockenstein E, Makriyannis A, et al. The cannabinoid CB_2 receptor agonist AM1241 enhances neurogenesis in GFAP/Gp120 transgenic mice displaying deficits in neurogenesis. Br. J. Pharmacol. 2014; 171: 468–479. https://doi.org/10.1111/bph.12478 PMID: 24148086

26. Barutta F, Piscitelli F, Pinach S, Bruno G, Gambino R, et al. Protective role of cannabinoid receptor type 2 in a mouse model of diabetic nephropathy. Diabetes. 2011; 60: 2386–2396. https://doi.org/10.2337/db10-1809 PMID: 21810593

27. Kamel AS, Abdelkader NF, Abd El-Rahman SS, Emara M, Zaki HF, et al. Stimulation of ACE2/ANG(1–7)/Mas Axis by Diminazene Ameliorates Alzheimer's Disease in the D-Galactose-Ovariectomized Rat Model: Role of PI3K/Akt Pathway. Mol Neurobiol. 2018; 55: 8188–8202. https://doi.org/10.1007/s12035-018-0966-3 PMID: 29516284

28. Khajuria DK, Razdan R, Mahapatra DR Description of a new method of ovariectomy in female rats. Rev Bras Reumatol. 2012; 52: 462–470. PMID: 22641600

29. Antunes M, Biala G The novel object recognition memory: neurobiology, test procedure, and its modifications. Cogn Process. 2012; 13: 93–110. https://doi.org/10.1007/s10339-011-0430-z PMID: 22160349

30. Alawdi SH, El-Denshary ES, Safar MM, Eidi H, David MO, et al. Neuroprotective Effect of Nanodiamond in Alzheimer's Disease Rat Model: a Pivotal Role for Modulating NF-κB and STAT3 Signaling. Mol Neurobiol. 2017; 54: 1906–1918. https://doi.org/10.1007/s12035-016-9762-0 PMID: 26897372

31. Suvarna SK, Layton C 5—The gross room/surgical cut-up. In: Suvarna SK, Layton C, Bancroft JD, editors. Bancroft's Theory and Practice of Histological Techniques (Seventh Edition). Oxford: Churchill Livingstone.2013. pp. 95–103.

32. Abd-ElRaouf A, Nada AS, Mohammed NEA, Amer HA, Abd-ElRahman SS, et al. Low dose gamma irradiation attenuates cyclophosphamide-induced cardiotoxicity in rats: role of NF-κB signaling pathway. Int J Radiat Biol. 2021; 97: 632–641. https://doi.org/10.1080/09553002.2021.1893856 PMID: 33635746

33. Ibrahim WW, Safar MM, Khattab MM, Agha AM 17β-Estradiol augments antidepressant efficacy of escitalopram in ovariectomized rats: Neuroprotective and serotonin reuptake transporter modulatory effects. Psychoneuroendocrinology. 2016; 74: 240–250. https://doi.org/10.1016/j.psyneuen.2016.09.013 PMID: 27685339

34. Anukulthanakorn K, Malaivijitnond S, Kitahashi T, Jaroenporn S, Parhar I Molecular events during the induction of neurodegeneration and memory loss in estrogen-deficient rats. Gen Comp Endocrinol. 2013; 181: 316–323. https://doi.org/10.1016/j.ygcen.2012.07.034 PMID: 23036734

35. Aydın AF, Küçükgergin C, Çoban J, Doğan-Ekici I, Doğru-Abbasoğlu S, et al. Carnosine prevents testicular oxidative stress and advanced glycation end product formation in D-galactose-induced aged rats. Andrologia. 2018; 50: e12939. https://doi.org/10.1111/and.12939 PMID: 29230838

36. Hua X, Lei M, Zhang Y, Ding J, Han Q, et al. Long-term D-galactose injection combined with ovariectomy serves as a new rodent model for Alzheimer's disease. Life Sci. 2007; 80: 1897–1905. https://doi.org/10.1016/j.lfs.2007.02.030 PMID: 17391708

37. Wang W, Li S, Dong HP, Lv S, Tang YY Differential impairment of spatial and nonspatial cognition in a mouse model of brain aging. Life Sci. 2009; 85: 127–135. https://doi.org/10.1016/j.lfs.2009.05.003 PMID: 19450612

38. Martín-Moreno AM, Brera B, Spuch C, Carro E, García-García L, et al. Prolonged oral cannabinoid administration prevents neuroinflammation, lowers β-amyloid levels and improves cognitive performance in Tg APP 2576 mice. J Neuroinflammation. 2012; 9: 8. https://doi.org/10.1186/1742-2094-9-8 PMID: 22248049

39. Franco R, Fernandez-Suarez D Alternatively activated microglia and macrophages in the central nervous system. Prog Neurobiol. 2015; 131: 65–86. https://doi.org/10.1016/j.pneurobio.2015.05.003 PMID: 26067058

40. Gu M, Li Y, Tang H, Zhang C, Li W, et al. Endogenous Omega (n)-3 Fatty Acids in Fat-1 Mice Attenuated Depression-Like Behavior, Imbalance between Microglial M1 and M2 Phenotypes, and Dysfunction of Neurotrophins Induced by Lipopolysaccharide Administration. Nutrients. 2018; 10: 1351.

41. Wang Y, He H, Li D, Zhu W, Duan K, et al. The role of the TLR4 signaling pathway in cognitive deficits following surgery in aged rats. Mol Med Rep. 2013; 7: 1137–1142. https://doi.org/10.3892/mmr.2013.1322 PMID: 23426570

42. Yang J, Wise L, Fukuchi K-i TLR4 Cross-Talk With NLRP3 Inflammasome and Complement Signaling Pathways in Alzheimer's Disease. Front Immunol. 2020; 11. https://doi.org/10.3389/fimmu.2020.00724 PMID: 32391019

43. Liu W, Huang S, Li Y, Zhang K, Zheng X Suppressive effect of glycyrrhizic acid against lipopolysaccharide-induced neuroinflammation and cognitive impairment in C57 mice via toll-like receptor 4 signaling pathway. Food Nutr Res. 2019; 63: https://doi.org/10.29219/fnr.v63.1516 PMID: 31073286

44. Xia C, Cao X, Cui L, Liu H, Wang S, et al. Anti-aging effect of the combination of Bifidobacterium longum and B. animalis in a d-galactose-treated mice. J Fun Foods. 2020; 69: 103938.

45. Bierhaus A, Humpert PM, Morcos M, Wendt T, Chavakis T, et al. Understanding RAGE, the receptor for advanced glycation end products. J Mol Med (Berl). 2005; 83: 876–886. https://doi.org/10.1007/s00109-005-0688-7 PMID: 16133426

46. Srikanth V, Maczurek A, Phan T, Steele M, Westcott B, et al. Advanced glycation endproducts and their receptor RAGE in Alzheimer's disease. Neurobiol Aging. 2011; 32: 763–777. https://doi.org/10.1016/j.neurobiolaging.2009.04.016 PMID: 19464758

47. Adhikary S, Li H, Heller J, Skarica M, Zhang M, et al. Modulation of inflammatory responses by a cannabinoid-2-selective agonist after spinal cord injury. J Neurotrauma. 2011; 28: 2417–2427. https://doi.org/10.1089/neu.2011.1853 PMID: 21970496

48. Aso E, Juves S, Maldonado R, Ferrer I CB2 cannabinoid receptor agonist ameliorates Alzheimer-like phenotype in AbetaPP/PS1 mice. J Alzheimers Dis. 2013; 35: 847–858. https://doi.org/10.3233/JAD-130137 PMID: 23515018

49. Burguillos MA, Deierborg T, Kavanagh E, Persson A, Hajji N, et al. Caspase signalling controls microglia activation and neurotoxicity. Nature. 2011; 472: 319–324. https://doi.org/10.1038/nature09788 PMID: 21389984

50. Du Z, Li S, Liu L, Yang Q, Zhang H, et al. NADPH oxidase 3-associated oxidative stress and caspase 3-dependent apoptosis in the cochleae of D-galactose-induced aged rats. Mol Med Rep. 2015; 12: 7883–7890. https://doi.org/10.3892/mmr.2015.4430 PMID: 26498835

51. Lu J, Wu DM, Zheng YL, Hu B, Zhang ZF Purple sweet potato color alleviates D-galactose-induced brain aging in old mice by promoting survival of neurons via PI3K pathway and inhibiting cytochrome C-mediated apoptosis. Brain Pathol. 2010; 20: 598–612. https://doi.org/10.1111/j.1750-3639.2009.00339.x PMID: 19863544

52. Jeong HJ, Kim SJ, Moon PD, Kim NH, Kim JS, et al. Antiapoptotic mechanism of cannabinoid receptor 2 agonist on cisplatin-induced apoptosis in the HEI-OC1 auditory cell line. J Neurosci Res. 2007; 85: 896–905. https://doi.org/10.1002/jnr.21168 PMID: 17183590

53. Viscomi MT, Oddi S, Latini L, Pasquariello N, Florenzano F, et al. Selective CB2 receptor agonism protects central neurons from remote axotomy-induced apoptosis through the PI3K/Akt pathway. J. Neurosci. 2009; 29: 4564–4570. https://doi.org/10.1523/JNEUROSCI.0786-09.2009 PMID: 19357281

54. Wang H, Xu J, Lazarovici P, Quirion R, Zheng W cAMP Response Element-Binding Protein (CREB): A Possible Signaling Molecule Link in the Pathophysiology of Schizophrenia. Front Mol Neurosci. 2018; 11. https://doi.org/10.3389/fnmol.2018.00255 PMID: 30214393

55. Cheng CY, Tang NY, Kao ST, Hsieh CL Ferulic Acid Administered at Various Time Points Protects against Cerebral Infarction by Activating p38 MAPK/p90RSK/CREB/Bcl-2 Anti-Apoptotic Signaling in the Subacute Phase of Cerebral Ischemia-Reperfusion Injury in Rats. PLoS One. 2016; 11: e0155748. https://doi.org/10.1371/journal.pone.0155748 PMID: 27187745

56. Zimbone S, Monaco I, Gianì F, Pandini G, Copani AG, et al. Amyloid Beta monomers regulate cyclic adenosine monophosphate response element binding protein functions by activating type-1 insulin-like growth factor receptors in neuronal cells. Aging Cell. 2018; 17. https://doi.org/10.1111/acel.12684 PMID: 29094448

57. Stucky A, Bakshi KP, Friedman E, Wang HY Prenatal Cocaine Exposure Upregulates BDNF-TrkB Signaling. PLoS One. 2016; 11: e0160585. https://doi.org/10.1371/journal.pone.0160585 PMID: 27494324

58. Colucci-D'Amato L, Speranza L, Volpicelli F. Neurotrophic Factor BDNF, Physiological Functions and Therapeutic Potential in Depression, Neurodegeneration and Brain Cancer. Int J Mol Sci. 2020; 21.

59. Isokawa M Time-dependent induction of CREB phosphorylation in the hippocampus by the endogenous cannabinoid. Neurosci Lett. 2009; 457: 53–57. https://doi.org/10.1016/j.neulet.2009.04.003 PMID: 19429161

60. Ferreira FF, Ribeiro FF, Rodrigues RS, Sebastião AM, Xapelli S Brain-Derived Neurotrophic Factor (BDNF) Role in Cannabinoid-Mediated Neurogenesis. Front Cell Neurosci. 2018; 12: 441–441. https://doi.org/10.3389/fncel.2018.00441 PMID: 30546297

61. Choi IY, Ju C, Anthony Jalin AM, Lee DI, Prather PL, et al. Activation of cannabinoid CB2 receptor-mediated AMPK/CREB pathway reduces cerebral ischemic injury. Am J Pathol. 2013; 182: 928–939. https://doi.org/10.1016/j.ajpath.2012.11.024 PMID: 23414569

62. Olsen M, Aguilar X, Sehlin D, Fang X, Antoni G, et al. Astroglial Responses to Amyloid-Beta Progression in a Mouse Model of Alzheimer's Disease. Mol Imaging Biol. 2018; 20(4): 605–614. https://doi.org/10.1007/s11307-017-1153-z PMID: 29297157

63. Nielsen HM, Mulder SD, Beliën JA, Musters RJ, Eikelenboom P, et al. Astrocytic A beta 1–42 uptake is determined by A beta-aggregation state and the presence of amyloid-associated proteins. Glia. 2010; 58: 1235–1246. https://doi.org/10.1002/glia.21004 PMID: 20544859

64. Beach TG, McGeer EG Lamina-specific arrangement of astrocytic gliosis and senile plaques in Alzheimer's disease visual cortex. Brain Res. 1988; 463: 357–361. https://doi.org/10.1016/0006-8993(88)90410-6 PMID: 3196922

65. Ewida FS, Mansour A. AM the antioxidant metabolic protective effect of exercise on d-galactose induced spatial memory impairment; possible role of hippocampal astrocytes. Al-Azhar Medical Journal. 2015; 44: 295–316.

66. Kemal S, Vassar R Death by microglia. J Exp Med. 2019; 216: 2451–2452. https://doi.org/10.1084/jem.20191536 PMID: 31645368

67. Gómez-Gálvez Y, Palomo-Garo C, Fernández-Ruiz J, García C Potential of the cannabinoid CB(2) receptor as a pharmacological target against inflammation in Parkinson's disease. Prog Neuropsychopharmacol Biol Psychiatry. 2016; 64: 200–208. https://doi.org/10.1016/j.pnpbp.2015.03.017 PMID: 25863279